Trends in water quality in a subtropical Australian river-estuary system: Responses to damming, climate variability and wastewater discharges

Trends in water quality in a subtropical Australian river-estuary system: responses to damming, climate variability and wastewater discharges

Rohan Eccles[a,*], Hong Zhang[a,*], David Hamilton[b], Paul Maxwell[c,d]

[a]*School of Engineering and Built Environment, Griffith University, Gold Coast Campus, QLD 4215, Australia*

[b]*Australian Rivers Institute, Griffith University, Nathan Campus, QLD 4111, Australia*

[c]*Healthy Land and Water, Brisbane, QLD 4000, Australia*

[d]*School of Chemical Engineering, University of Queensland, QLD, 4072, Australia*

Abstract:

The Logan-Albert estuary in southeast Queensland, Australia, has high biodiversity and supports multiple economic and recreational services. Elevated nutrient and sediment loads have been a longstanding management issue for the estuary. We investigated the spatial and seasonal patterns of nutrients and turbidity along the Logan-Albert estuary and assessed the effects of a recently constructed upstream dam. Nutrient concentrations and turbidity levels were analysed using 15 years of monitoring data from 19 water quality sites throughout the estuary. We hypothesised that the construction of Wyaralong Dam would act as a nutrient and sediment sink which may have positive effects on downstream water quality. Long-term trends of water quality constituents were evaluated using a non-parametric seasonal Mann-Kendall test and the effect of upstream impoundment was assessed with a Before-After Control-Impact (BACI) test. Nutrient concentrations and turbidity levels declined significantly with time in the upper Logan estuary and, to a lesser extent, in the lower Albert estuary. The general improvement of water quality in the upper Logan estuary was attributed to construction of the Wyaralong Dam. Significant decreases in concentrations of total phosphorus (TP) and oxidised nitrogen (NO_x-N) along the lower Albert were principally attributed to wetter conditions over the 15-year dataset, which diluted point-source loads from a nearby wastewater treatment plant (WWTP). Our results show that estuarine water quality changes can be highly dynamic with interactions amongst climate and management practices that necessitate long-term monitoring programs with good spatial coverage.

Keywords: Monitoring, Trend analysis, Water quality, Dam, Subtropical, Estuary

1. Introduction

Surface water pollution from elevated sediment and nutrient loads has become an important environmental issue, leading to eutrophication and decreased biodiversity (Rabalais et al., 2009). Levels of nutrients and sediment are often used as a proxy for river and estuary health, to assess the impacts of anthropogenic changes, and underpin the implementation of management strategies to mitigate adverse changes (Li et al., 2018; Medeiros et al., 2011). Limited understanding of the long-term trends and drivers of water quality change may lead to poor decision making about possible management strategies (Bertone et al., 2015). Disentangling these complex interactions between anthropogenic and natural drivers of change, which may act synergistically or antagonistically, remains a major challenge for managers, particularly in highly variable subtropical climates.

Over the last century, the seasonal regime of nutrient and sediment loads has been significantly altered in many rivers (Malmqvist and Rundle, 2002; Walling and Fang, 2003). Widespread deforestation, and agricultural and urban development are some of the principal factors which have led to excessive nutrient and sediment loads to downstream ecosystems (Malmqvist and Rundle, 2002). The effects of climate change, particularly changes in rainfall variability and intensity, may further increase loads (Molina-Navarro et al., 2018; Nunes et al., 2009; Shrestha et al., 2017). Conversely, the construction of dams and weirs, which alter natural flow patterns of rivers, can reduce downstream sediment and nutrient loads (Walling and Fang, 2003). Dams can effectively trap particulate nutrients and sediments, particularly in the early stages following construction (Friedl and Wüest, 2002; Medeiros et al., 2011; Zhang et al., 2013). Phosphorus adsorption to inorganic particles and denitrification within dams may also attenuate the export of nutrients. It has been argued that the impact of dams on downstream river flows and water quality may be greater in Australia than elsewhere in the world, due to greater climatic variability and highly variable flow regimes of Australian rivers (Harris, 2001).

Before-After Control-Impact (BACI) design is a statistically powerful design tool suitable for environmental impact studies where a particular causal factor may be implicated in an environmental change (Stewart-Oaten et al., 1986). It effectively separates the influence of natural variability from anthropogenic disturbances, providing that adequate data are collected and the timing of the impact is known (Smokorowski and Randall, 2017). The BACI approach has been adopted for a range of environmental impact studies, including assessing the effects of reservoir removal and impoundment (Chang et al., 2017; Martina et al., 2013), stream morphology changes (Hughes and Quinn, 2014; Thompson et al., 2018), and wastewater treatment plant (WWTP) upgrades (Dąbrowska et al., 2017).

Water quality measurements, taken predominantly on a monthly basis and available for numerous sites throughout the Logan-Albert estuary, were used in this study to investigate river-estuarine water quality, both spatially and temporally. The aims of this study were to (1) identify the mechanisms driving the spatial and seasonal patterns of nutrient concentrations and turbidity, (2) detect the long-term trends for these constituents, and (3) evaluate the effects of the recently constructed Wyaralong Dam on downstream water quality using the BACI design. We hypothesised that the construction of the upstream Wyaralong Dam would be detected as a positive impact for downstream water quality, superseding other negative environmental drivers relating to ongoing land use change, and dominating other possible drivers related to climate change and variability.

2. Study site, historical data and sample collection

The study was focussed on the Logan-Albert river estuary (Fig. 1), located south of Brisbane in southeast Queensland. The estuary supports a wide diversity of aquatic life and is important economically and recreationally. The system has a catchment area of approximately 3862 km^2, of which the Logan River catchment covers around 3080 km^2 and the Albert 782 km^2. The Logan and Albert Rivers rise along the McPherson ranges and converge approximately 11.1 km from the river mouth. The estuary discharge is to the Ramsar listed wetlands of southern Moreton Bay. The bay experiences semidiurnal microtidal (range <2 m) and mesotidal (range 2-4 m) conditions with a maximum range of 2.8 m (Tibbetts et al., 1999). The tidal influence extends approximately 60 km upstream on the Logan River and 35 km upstream of the Logan River confluence on the Albert River. Flood current velocities and duration exceed those of the ebb tide (Mirfenderesk and Tomlinson, 2006) and typical flushing times range from 66 to 75 days (Dennison and Abal, 1999).

The southeast Queensland region has experienced a significant deterioration in water quality since arrival of European people in 1823 (Olley et al., 2015) and the ecological decline of the major coastal receiving waters of Moreton Bay has been attributed to increased nutrient and sediment loads from the rivers in the region (Abal et al., 2005; Bunn et al., 2007). It is estimated that phosphorus and nitrogen loads from the Logan-Albert river system have increased by a factor of 4.7 and 3.2, respectively, and sediment loads by a factor of 35 since European arrival (National Land and Water Resources Audit, 2001). The Logan-Albert catchment has been identified by the Department of Infrastructure and Transport (2013) as an area for major urban expansion, which may stress the already-degraded estuary system.

At the same time the effects of Wyaralong Dam, constructed upstream of the Logan River in 2010 have not yet been established. It was built to supplement the drinking water supplies for southeast Queensland following a major drought across south-eastern Australia in 2001-2009 (van Dijk et al., 2013). The dam has a storage capacity of 103,000 ML and a catchment of 546 km^2. Construction of the dam coincided with a change in the predominant meteorological conditions, from prolonged drought to wetter conditions culminating in major rainfall events in January 2011, January 2013, and April 2017, which led to the dam filling almost immediately after impoundment.

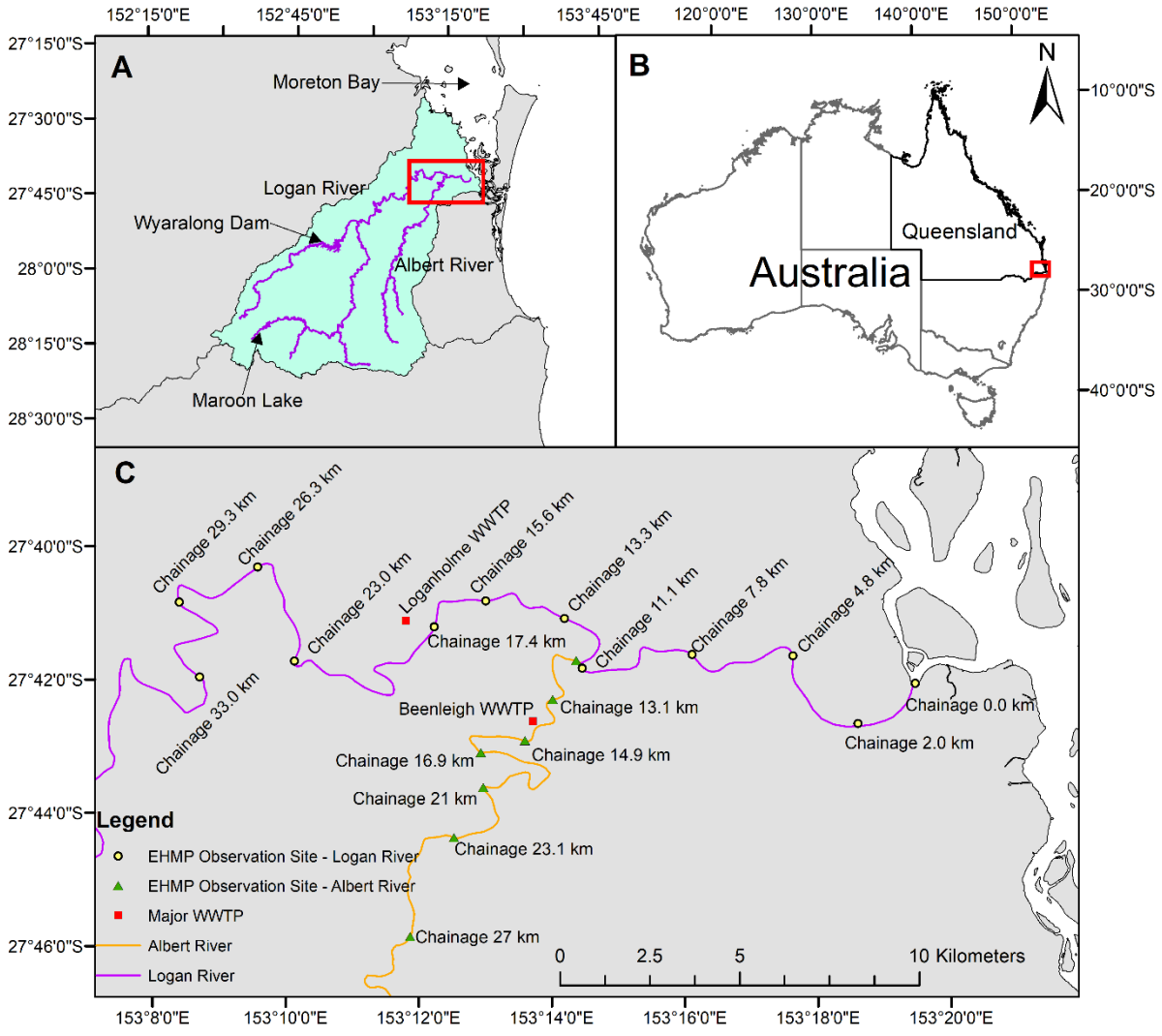

Fig. 1. A) Location of the study area and major dams within the Logan-Albert catchment, B) location of catchment within Australia, C) location of Ecosystem Health Monitoring Program (EHMP) water quality monitoring sites, associated chainages from the river mouth, and the positions of the two major wastewater treatment plants (WWTPs) within the catchment.

Annual rainfall across the Logan-Albert catchment is spatially and temporally variable, ranging from 800 mm in the southwest to over 2000 mm in the south-eastern headwaters. A distinct wet season occurs in summer and a dry season in winter. Catchment headwater land use is dominated by native forest and scrub and by cattle grazing and pastoral lands in the upper to mid catchment, with irrigated cropping along the alluvial channels. Intensive dairies, poultry farms, horse studs, turf farms and hoop pine plantations occur in parts of the upper and middle catchment (DSITIA2014). Urban and rural residential developments are located across the lower catchment. Logan City, located along the upper estuary, is the largest population centre with approximately 319,000 residents (Queensland Government Statistician's Office, 2018). Two major WWTPs are located close to this population centre and release effluent into the Logan and Albert estuaries at Chainage 17 and 15.1 km, respectively (Figure 1; DEHP2015). Treatment at the Logan WWTP involves either oxidation or biological nutrient removal through bioreactors followed by secondary clarifiers. At the Albert WWTP, biological nutrient removal is followed by clarification. The lower catchment comprises of large areas of sugarcane farming along the southern floodplains (Chainage 11.1 to 0 km).

Water quality monitoring data were obtained from the Ecosystem Health Monitoring Program (EHMP2007). EHMP conducts water quality sampling during ebb tides approximately 2 hours after high tide at twelve sites in the Logan estuary and seven in the Albert estuary (Fig. 1). Sampling was conducted from the river mouth to the extent of tidal influence, approximately 33 and 27 km upstream for the Logan and Albert estuaries, respectively. Water quality data were assessed between 2003 and 2018 for all sites. From 2003 to 2014, sampling was monthly, after which the sampling frequency was reduced to eight times annually, by excluding sampling in January, April, June and July.

Turbidity was measured with a YSI 6920 turbidity sensor (Yellow Springs Instruments, Ohio). Nutrient samples were taken just below the water surface, filtered on site, and transported on ice until return to the laboratory where they were kept frozen until analysis. Filtered samples were analysed for filterable reactive phosphorus (FRP), ammonium (NH_4-N), nitrate (NO_3-N), and nitrite (NO_2-N) using an automated LACHAT 8000QC flow injection analyser (FIA; American Public Health Association, 1998). Unfiltered samples were digested in an alkaline persulphate solution and analysed for TN and TP using the FIA, i.e., as FRP and NO_3-N following the digestion (American Public Health Association, 1998).

The Queensland Department of Natural Resources, Mines and Energy regularly measures streamflow and water levels at several monitoring sites in the Logan-Albert catchment. River inflow from the Yarrahappini and Bromfleet stream gauges (ID: 145014A and 145102B) were

applied in this study as they were closest to the tidal limit of the Logan-Albert estuary. Annual average loads of NH_4-N, TN and TP to the estuary from the two major WWTPs (Fig. 1) were retrieved from the National Pollutant Inventory (NPI2019).

3. Methods

3.1. Data pre-processing

A small number of measured nutrient concentrations were below the detection limit (~0.002 mg/L for NH_4-N (10% of samples), NO_x-N (5.2%), and FRP (0.18%), and 0.01 mg/L for TP (0.18%)). They were replaced using:

$$c_{ki} = d_k R_{ki} \quad (1)$$

where c_{ki} is the estimated concentration for the k^{th} variable at the i^{th} timestep, d_k is the detection limit for variable k, and R_{ki} is a uniformly distributed random number between 0.01 and 0.99 such that the mean of all censored values for each variable would be approximately half the detection limit. When sampling involved numerous measurements taken at the water surface for a single day, the averaged concentration was applied in these analyses. There were a small number of missing datapoints for some constituents at some locations but as this number was small (<4%) we chose to include all datapoints for these analyses.

3.2. Seasonal and spatial analysis

Monthly boxplots of TN and TP concentrations, turbidity, streamflow, salinity, and water temperature were calculated for the most upstream sampling sites: Logan (Chainage 33 km) and Albert (Chainage 27 km), where chainage is the adopted middle thread distance from the river mouth. Median monthly water quality values were calculated for salinity and all water quality constituents, at all sites. Median values were utilised instead of means to reduce the effects of extreme values. Similarly, median TN:TP, FRP:TP, and NO_x-N:TN mass ratio values were calculated for all sites and months. This analysis allowed for inferences to made on whether the system may be N or P limited based on the Redfield molar element ratio of 16:1 for N:P or approximately 7:1 for mass. Mass ratios of TN:TP < 7 were inferred to be indicative of N limitation.

3.3. Trend analysis

Trends between 2003 and 2018 were evaluated with the seasonal Mann-Kendall test (Hirsch et al., 1982) for all constituents at all sites. This method has been widely adopted to

assess monotonic trends in environmental time-series due to its robust nature and ability to consider non-normally distributed data, making it ideal for environmental and streamflow data (Li et al., 2018). A significance level of 0.01 was used in these tests to denote a highly significant trend. The results of the Mann-Kendall test were compared to those from a Generalised Additive Model (GAM) approach (Murphy et al. 2019). Details of the GAM methodology are given in Section S2 of the Supplementary Materials. Optimal change points were detected for the timeseries using a minimalised cost function in MATLAB to investigate if their position through time coincided with the impoundment of Wyaralong Dam.

3.4. Impact assessment

Delineating the effects of Wyaralong Dam on nutrient concentrations and turbidity from other effects was done by implementing a BACI design (Stewart-Oaten et al., 1986). This test controls for natural variability by comparing water quality samples at both control and impact sites taken at the same time (Smith, 2002). An 'impact' site was selected as the most upstream site along the Logan estuary (Chainage 33 km) where the effects of upstream impoundment are likely to be greatest. The upstream Albert estuary site (Chainage 27 km) was selected as the 'control'. Both sites are located in similar along-river positions with similar degrees of saline intrusion (Fig. 2 and Fig. 3). Samples taken at the control and impact sites were paired when sampling occurred on the same day, or excluded when they did not. The differences between paired data points were calculated for the before and after impoundment periods as:

$$D_{ik} = X_{iC_k} - X_{iI_k} = \mu + \eta_i + \varepsilon_{ik} \quad (2)$$

where, D_{ik} is the difference between the before and after period i, for the k^{th} paired value, X denotes the variable of interest, with C and I indicating either control or impact sites, μ is the mean difference, η_{i} is the change in difference before and after impoundment, and $\varepsilon_{\mathrm{ik}}$ is the error from these differences (Smith, 2002). The pre-impoundment period included all sampling that occurred before the diversion channel was plugged and the dam began to fill (December 2010) and the post-impoundment period included all sampling thereafter. The calculated differences (D_{ik}) are required to meet the assumption of additivity and independence. Additivity was tested by comparing a non-zero slope of the regression of differences (D_{ik}) against the mean observed value between impact and control sites, while independence was evaluated using the Durbin Watson test (Smokorowski and Randall, 2017; Stewart-Oaten et al., 1986). All observation data were natural log transformed prior to performing the BACI test, to better meet the assumption of additivity. As the transformed water quality data used in this

analysis did not all meet parametric conditions, the non-parametric Wilcoxon Rank Sum test was applied. We tested for a null hypothesis that there was no difference between each of the pre- and post-impoundment median water constituent values.

To evaluate the magnitude of change between the Before (pre-impoundment) and After (post-impoundment) groupings the Hodges-Lehmann estimator of step trend magnitude (Hodges Jr and Lehmann, 1963) and associated 95% confidence intervals were calculated for all sites and variables. The estimator was used to calculate the absolute and percentage changes in water quality constituents relative to the pre-impoundment period.

4. Results

4.1. Seasonal and spatial patterns

Inflows to the Logan and Albert estuaries showed clear seasonal trends. There was significant year-to-year variability for wet season flows (November to April) evident by the large interquartile ranges for these months, whereas dry season flows (May to October) were consistent throughout the study period, with smaller interquartile ranges (Fig. 2). Median water temperatures in the upper estuaries peaked in summer at 27.2 °C (January) and were lowest in winter at 15.3 °C (July). Salinity levels typically remained low throughout most of the year, except for a discernible peak in concentrations at the end of the dry season/start of the wet season (October). At the upper Albert estuary site, TN, TP, and turbidity generally followed the seasonal patterns of streamflow, with higher levels recorded during the wet season. However, this seasonality was much less evident at the upper Logan estuary site. Instead, constituent concentrations at this location showed much greater year-to-year variation for all months compared to the Albert site, particularly during the dry season.

Longitudinal profiles of monthly median water quality values over the sampling period are shown in Fig. 3. Salinity followed a similar seasonal pattern to that seen in Fig. 2 throughout the estuary, with peak concentrations occurring at the end of the dry season/start of the wet season and lowest concentrations coinciding with the end of the wet season. Values of TN, TP, and turbidity are similar to those in Fig. 2, but the degree of seasonality is much more pronounced for TN and TP along the Albert estuary compared to the Logan. For NH_4-N concentrations the pattern is reversed, with higher values recorded during the dry season, especially at the sites in close proximity to the two major WWTPs located at Chainage 17 and 15.1 km along the Logan and Albert estuaries, respectively. Monitoring sites upstream of the WWTPs had higher FRP concentrations during wet-season months, while sites near to, and downstream of the WWTPs typically had higher concentrations during the dry season for both

systems. Concentrations of NO_x-N did not show any clear seasonal patterns along the length of either estuary.

Annual median nutrient concentrations were highest along the lower reaches of the Albert between the WWTP site and the confluence with the Logan River (Chainage 13.1 to 14.9 km). Concentrations of TN and TP peaked further upstream along the Logan, around Chainage 23 km. In the Logan, peak concentrations of NH_4-N, NO_x-N, and FRP all coincided with the location of the WWTP at Chainage 17.4 km. There were large increases in annual median turbidity (68 NTU) in the middle part of the Logan estuary between Chainages 17.4 (42 NTU) and 23 km (110 NTU). For the Albert, turbidity was highest in the mid estuary, though levels were less than half of those in the upper Logan. Maximum concentrations of all constituents were lower along the Albert compared to the Logan.

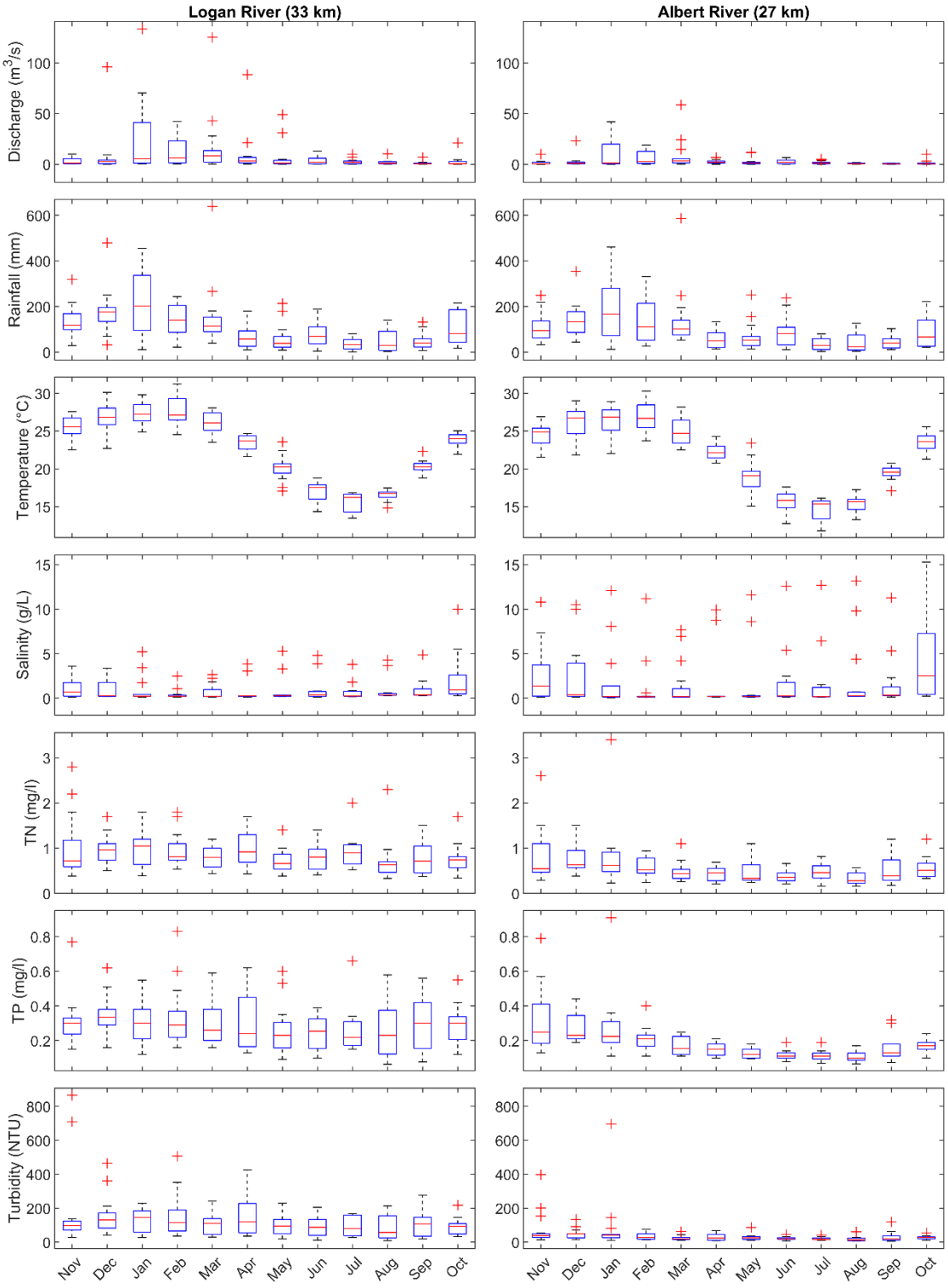

Fig. 2. Seasonal distribution of monthly mean streamflow, rainfall, water temperature, salinity, TN, TP, and turbidity in the upper Logan estuary (Chainage 33 km) and the upper Albert estuary site (Chainage 27 km) between 2003 and 2018.

Large differences in constituent values occurred seasonally. For example, in the middle Logan (Chainage 23 km) and Albert estuaries (Chainage 16.9 km) median turbidity ranged

from 55.4 (August) to 190.5 NTU (January) and 23 (August) to 100.3 NTU (November), respectively. Similarly large differences in NH_4-N concentrations occurred at sites closest to the two major WWTPs; 0.0235 (March) to 0.21 mg L^{-1} (September) for the Logan (Chainage 17.4 km) and 0.0295 (March) to 0.12 mg L^{-1} (August) for the Albert (Chainage 14.9 km), i.e., nearly an order of magnitude change at the site within the Logan but somewhat less at the site within the Albert.

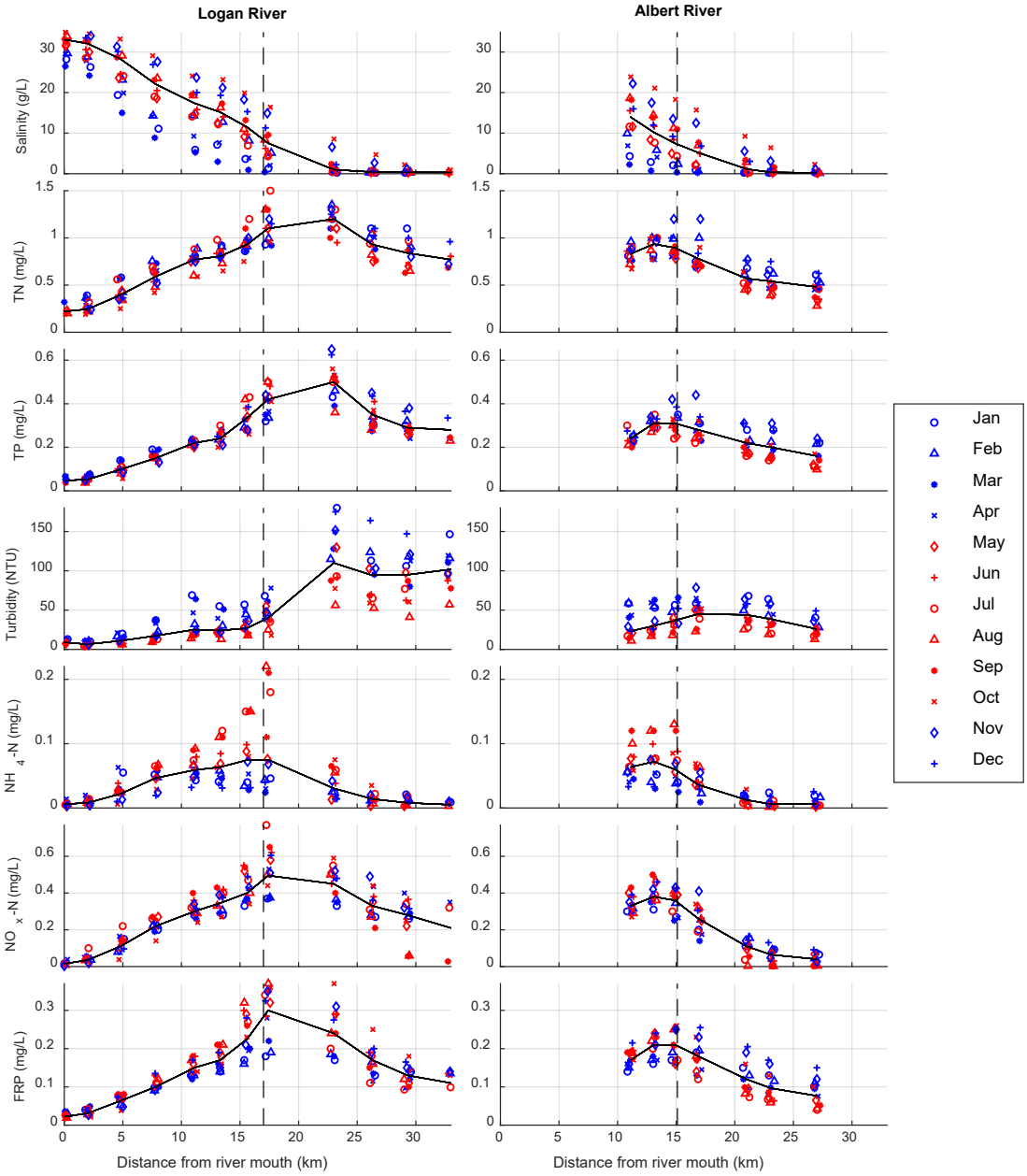

Fig. 3. Median values of key water quality constituents and salinity for all months along both estuaries during the sampling period (2003 – 2018) with increasing distance from the river mouth (Chainage 0 km). Black dashed lines show the locations of the two major WWTPs, blue points denote wet season months, red points show dry season months, and black solid lines show medians for all months.

Longitudinal profiles of TN:TP mass ratios (Fig. 4) were approximately inversely related to longitudinal profiles of TN and TP concentrations (Fig. 3), in that they were highest at the river mouth and steadily decreased to their lowest level around the location of maximum TN and TP concentrations. There was no clear seasonal pattern in TN:TP along the length of the Logan estuary, whereas along the Albert estuary ratios were greater during the dry season. This observation (for the upper estuary) suggests that TN is mobilised in greater relative quantities during the dry season and TP during the wet season in the Albert catchment. Both estuaries appear to be N-limited over their full length (based on TN:TP < 7), with the greatest N limitation occurring upstream in the riverine part and the lowest downstream where mixing occurs with waters of oceanic origin. Maximum FRP:TP and NO_x-N:TN ratios occurred around the location of the two WWTPs and FRP:TP ratios upstream of these WWTPs were considerably lower than those downstream. There was a noticeable seasonality of ratios near to and downstream of these WWTPs, with greater values recorded during the dry season.

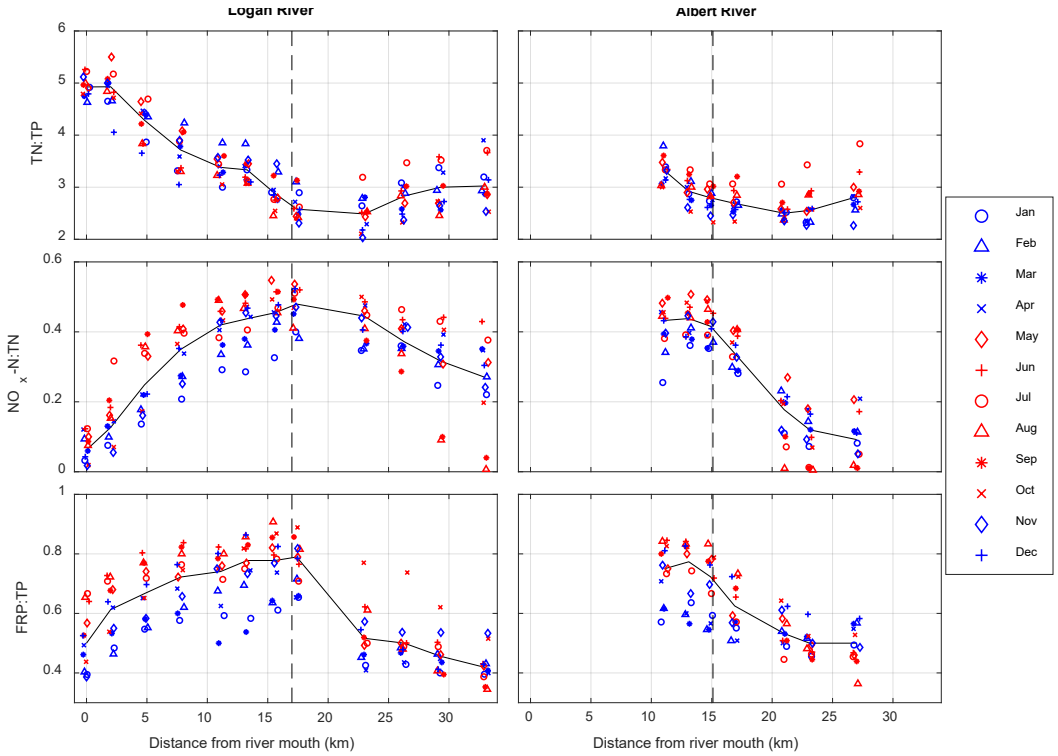

Fig. 4. Median TN to TP, NO_x-N to TN, and FRP to TP mass ratios for the length of the Logan and Albert estuaries during the sampling period (2003 – 2018).

4.2. Trends

Long-term trends for TN, TP, and turbidity for the upper Logan and Albert estuaries and for sites near the WWTPs are presented in Fig 5. Significant ($p<0.01$) downward trends with time were identified (seasonal Mann-Kendall test) for TN at all sites and for TP at all sites except for the upper Albert estuary (Chainage 27 km). For turbidity only the upper Logan estuary site had a significant downward trend over the study period. Calculated change points for TN (February to March 2012) and turbidity (February to July 2012) at all sites corresponded closely with when effects might have been expected from the impoundment of Wyaralong Dam (December 2010). While for TP the change points (January 2008 and November 2004) were seemingly unrelated to the opening of the dam.

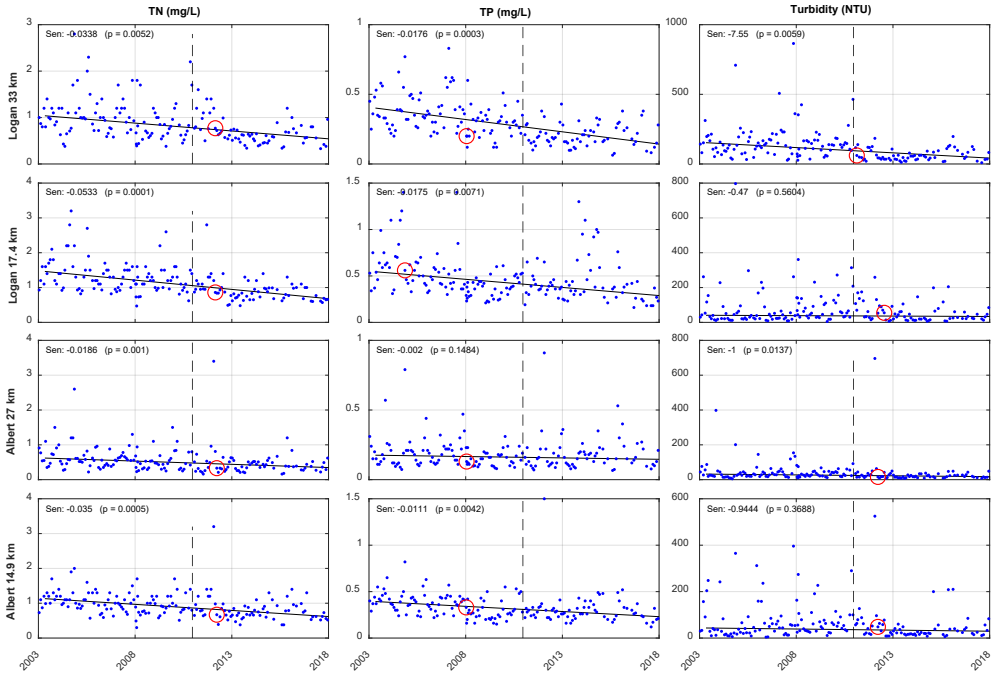

Fig. 5. Trend analysis of TN, TP, and turbidity between 2003 and 2018 (Logan Chainage 33 and 17.4 km and Albert Chainage 27 and 14.9 km) using the seasonal Mann-Kendall test (Sen's slope and significance level are provided for each plot). Vertical dashed black lines show the date of Wyaralong Dam impoundment and red circles show a change point determined from a cost minimised function.

Comparisons of the Sen's slope showed a downward trend for TN at most sites during the study period (Table 1). Only sites located within 11 km of the river mouth did not have a significant decrease. Rather, sites near to the river mouth presented an opposing trend of increasing TN and turbidity, but none of the slopes were significant ($p>0.01$). In contrast to TN, only two locations along the upper Logan estuary (Chainage 29.3 and 33 km) had significant ($p<0.01$) declines in turbidity. Decreases in TP and NO_x-N concentrations were

greatest along the upper and middle Logan estuary (Chainage 7.8 – 33 km) and along the lower Albert estuary (below Chainage 16.9 km). For NH_4-N, and FRP sites along the upper Logan estuary (Chainage 15.6 – 33 km) had significant downward trends ($p<0.01$), while no sites along the Albert showed any change through time ($p>0.01$). Only the upstream Albert site (Chainage 27 km) showed a significant increase ($p<0.01$) in FRP:TP ratios and a significant decrease in TN:TP ratios during the study period. There were significant ($p<0.01$) decreases in NO_x-N:TN ratios with time at all sites along the middle and upper Logan estuary (Chainage 7.8 – 33km) except for the site nearest to the WWTP (Chainage 17.4 km). While, only the most downstream site reported a significant ($p<0.01$) downward trend for the Albert estuary. Results from the GAM test (refer to Section S2 in the Supplementary Materials) were similar to those from the seasonal Mann-Kendall test. Though, the GAM results show significant downward trends at more sites than the Mann-Kendall test, especially for FRP (17 or 12 sites, depending on the number of selected for the analysis compared to 5 sites from the Mann-Kendall test).

Table 1. Trend analysis of all water quality constituents and mass ratios for all sites between 2003 and 2018 using the seasonal Mann-Kendall test. Sen's slope values are shown (average yearly change of variable, where greater positive and negative values indicated more pronounced positive and negative trends, respectively). Green background colours denote decreasing trends and red increasing trends, darker backgrounds represent lower p-values, and bold values indicate significant ($p<0.01$) trends.

Site (km)	TN	TP	Turbidity	NH_4-N	NO_x-N	FRP	TN:TP	FRP:TP	NO_x-N:TN
Logan 0	0.005	0.001	0.050	0.000	0.000	0.000	0.002	-0.005	0.000
Logan 2	0.003	0.000	0.193	0.000	0.000	-0.001	0.012	-0.010	-0.003
Logan 4.8	0.000	0.000	0.150	0.000	-0.003	0.000	0.019	-0.002	-0.007
Logan 7.8	-0.008	-0.002	0.245	0.000	**-0.010**	-0.002	0.005	-0.001	**-0.011**
Logan 11.1	-0.018	**-0.006**	-0.164	-0.001	**-0.015**	-0.004	0.000	-0.003	**-0.010**
Logan 13.3	**-0.023**	**-0.007**	-0.318	-0.002	**-0.017**	-0.005	0.004	0.001	**-0.009**
Logan 15.6	**-0.040**	**-0.014**	0.014	**-0.005**	**-0.030**	**-0.013**	0.002	-0.007	**-0.012**
Logan 17.4	**-0.053**	**-0.018**	-0.470	**-0.006**	**-0.038**	-0.017	-0.027	-0.006	-0.011
Logan 23	**-0.087**	**-0.035**	-7.938	**-0.003**	**-0.056**	**-0.022**	0.008	-0.006	**-0.020**
Logan 26.3	**-0.060**	**-0.027**	-6.100	**-0.001**	**-0.038**	**-0.015**	0.029	-0.004	**-0.024**
Logan 29.3	**-0.042**	**-0.020**	**-6.667**	0.000	**-0.028**	**-0.010**	0.057	-0.004	**-0.020**
Logan 33	**-0.034**	**-0.018**	**-7.550**	0.000	**-0.020**	**-0.007**	0.049	0.000	**-0.016**
Albert 11.1	-0.021	**-0.006**	-0.333	-0.002	**-0.016**	-0.005	0.000	-0.002	**-0.009**
Albert 13.1	**-0.030**	**-0.010**	-0.429	-0.002	**-0.023**	-0.009	0.003	-0.003	-0.010
Albert 14.9	**-0.035**	**-0.011**	-0.944	-0.002	**-0.023**	-0.008	-0.005	0.000	-0.011
Albert 16.9	**-0.027**	**-0.010**	-1.067	-0.001	-0.015	-0.005	-0.016	0.000	-0.009
Albert 21	**-0.020**	-0.005	-1.600	0.000	-0.004	-0.001	-0.038	0.006	-0.002
Albert 23.1	**-0.020**	-0.003	-1.600	0.000	0.000	0.000	-0.048	0.010	0.000
Albert 27	**-0.019**	-0.002	-1.000	0.000	0.000	0.002	**-0.084**	**0.015**	0.000

Annual reported nutrient loads (TN, TP, and NH_4-N) released from the Logan WWTP site to the stream displayed a decreasing trend over the study period (Fig. 6). For the Albert WWTP, only NH_4-N loads showed a decreasing trend, whereas TP loads remained mostly unchanged and TN loads increased. Over this same time period there was an increase in the monthly mean inflows along both rivers as evident by the positive Sen's slope values, though not at significant levels ($p>0.01$; Fig. 6). Interestingly, TN and TP concentrations showed significant ($p<0.01$) downward trends at the monitoring site (Chainage 14.9 km) closest to the WWTP in the Albert River despite loads either increasing or remaining unchanged, while NH_4-N concentrations did not change despite the reported decrease in loads (Table 1). All variables showed significant ($p<0.01$) decreases in concentration with time at the monitoring site (Chainage 17.4 km) closest to the WWTP on the Logan River.

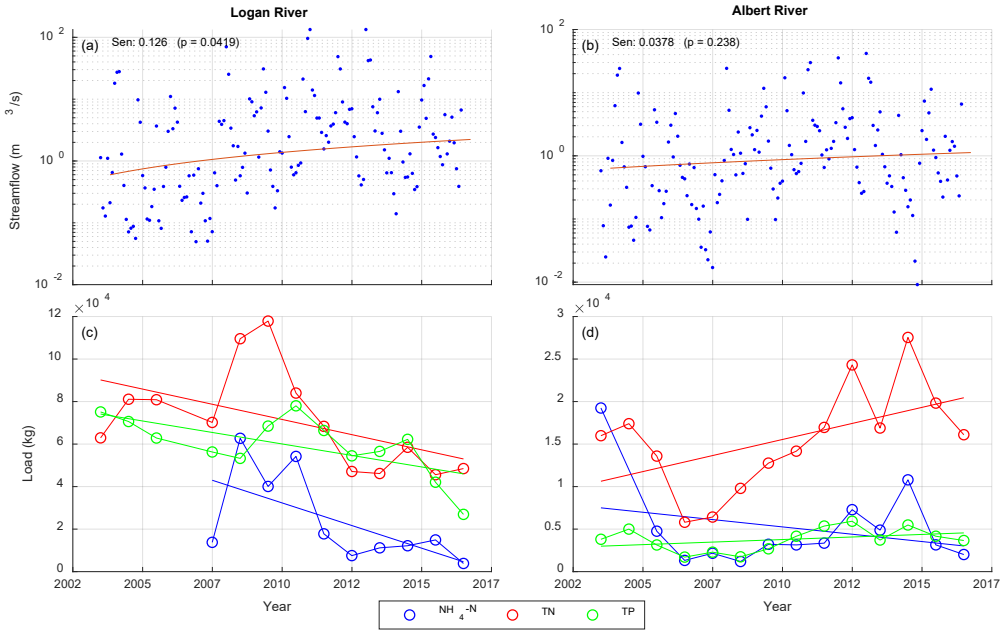

Fig.6. Monthly mean streamflow and trend using the seasonal Mann-Kendall test (Sen's slope and significance level are shown) for flows entering (a) the Logan estuary from the Yarrahappani gauge and (b) the Albert estuary from the Bromfleet gauge. National Pollutant Inventory (NPI) yearly reported nutrient loads discharged to stream from the two wastewater treatment plants (WWTPs) situated along (c) the Logan estuary at Chainage 17 km and (d) the Albert estuary at Chainage 15.1 km.

4.3. Impact of Wyaralong Dam

Boxplots of key water quality variables for pre- and post-impoundment periods are shown for the upper Logan and Albert estuaries and sites near the WWTPs (Fig. S1). Significant ($p<0.01$) differences in TN were found between these periods at all these sites. For TP and turbidity all sites except the upper Albert site (Chainage 27 km) and Logan WWTP site

(Chainage 17.4 km) showed significant ($p<0.01$) decreases. The largest changes occurred at the upper Logan estuary site for TP and turbidity and at the WWTP site on the Logan estuary for TN.

Significant decreases ($p<0.01$) in the post-impoundment period were detected at the upper Logan (impact) site for turbidity, TP, FRP, and NO_x-N using the BACI test (Table 2). Mean values for all constituents decreased at the impact site between the pre- and post-impoundment periods, while at the control site mean values of TP and FRP both increased. The standard deviation of all water quality constituents at the impact site also decreased considerably after impoundment, whereas it increased for four of the six variables (TN, TP, turbidity, and FRP) at the control site (Table 2).

Differences between pre- and post-impoundment periods, as assessed with the Hodges-Lehmann estimator and the corresponding percentage change in median values, are presented in Table 3 for both the control and impact sites. Turbidity showed the greatest decline post-impoundment (56.1% at the impact site and 33.3% at the control site). Large decreases in median values were also found for TP, NO_x-N, and FRP at the impact site (between 34.6 and 48.9%), whereas the changes were more modest at the control site (between 6.2 and 19.3%). For TN, decreases were similar at both sites (~27%). In contrast to all the other water quality constituents, NH_4-N concentrations decreased more at the control site than the impact site (26.1% compared to 0%).

Table 2. Monthly mean values with standard deviations in parentheses at the upper Logan and Albert estuary sites before and after impoundment. p-values are calculated from the BACI analysis using the Wilcoxon Rank Sum test and significant values are shown in bold.

Parameter	Logan 33 km (impact)		Albert 27 km (control)		p-value
	Before	After	Before	After	
TN (mg/L)	0.99 (0.44)	0.69 (0.27)	0.60 (0.35)	0.47 (0.41)	0.2853
TP (mg/L)	0.352 (0.133)	0.209 (0.084)	0.183 (0.106)	0.188 (0.126)	**<.01**
Turbidity (NTU)	158.2 (128.2)	65.2 (41.7)	42.6 (50.8)	33.8 (83.8)	**<.01**
NH_4-N (mg/L)	0.018 (0.035)	0.013 (0.020)	0.030 (0.075)	0.011 (0.016)	0.9741
FRP (mg/L)	0.148 (0.068)	0.096 (0.049)	0.084 (0.053)	0.104 (0.061)	**<.01**
NO_x-N (mg/L)	0.340 (0.283)	0.175 (0.174)	0.089 (0.127)	0.059 (0.076)	**<.01**

Table 3. Hodges-Lehmann estimators of nutrients (mgL^{-1}) and turbidity (NTU) for the Impact and Control sites and the associated percentage change (%) in parentheses using Before-After groupings. Negative values indicate a decrease in the median between the pre- and post-impoundment periods.

Site	TN	TP	Turbidity	NH_4-N	NO_x-N	FRP
Logan 33 km (Impact)	-0.25 (-27.2)	-0.13 (-39.4)	-76.9 (-56.1)	0 (0)	-0.137 (-48.9)	-0.045 (-34.6)
Albert 27 km (Control)	-0.15 (-27.5)	-0.01 (-6.2)	-9.5 (-33.3)	-0.003 (-26.1)	-0.01 (-17.4)	+0.014 (+19.3)

Calculated Hodges-Lehman estimators and percentage changes relative to pre-impoundment medians of water quality variables are presented in Fig. 7 for all sites. The largest decreases between the pre- and post-impoundment periods generally occurred along the upper and middle Logan estuary, while downstream sites showed little change. For the Albert estuary, the largest decreases in nutrients were downstream, close to the confluence with the Logan River. Turbidity decreased the most along the upper and middle sections of the Logan and Albert estuaries, respectively. The largest decreases in NH_4-N concentrations coincided with the locations of WWTPs for both estuaries. Relative changes to TP, FRP, turbidity, and NO_x-N were greatest in the upper Logan estuary and along the lower Albert estuary.

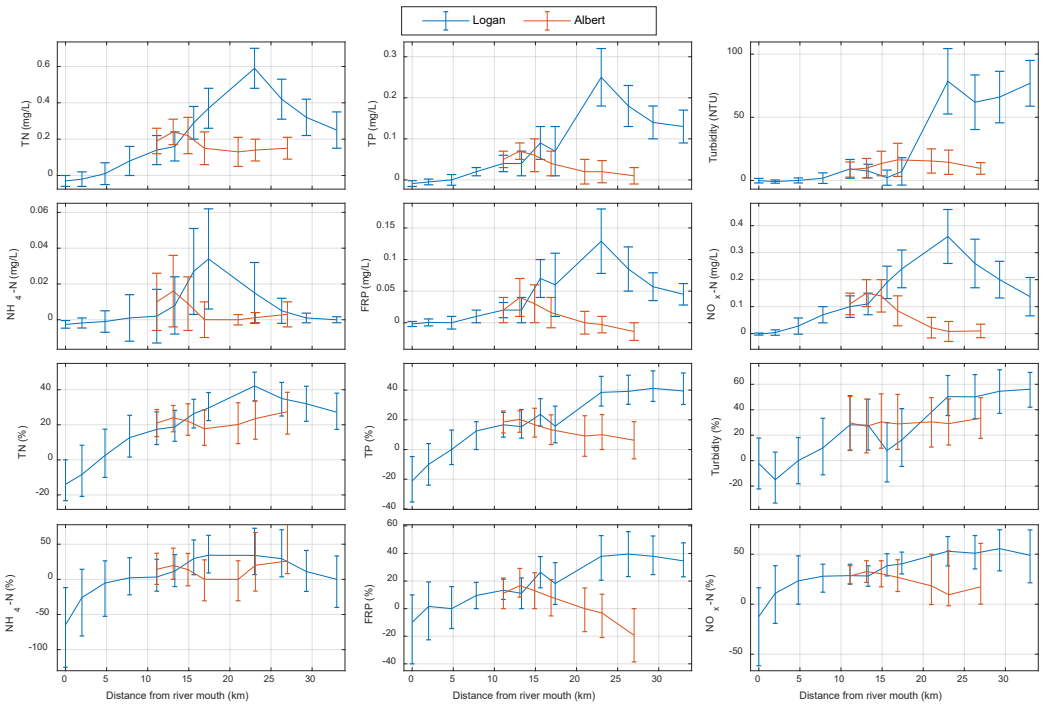

Fig.7. Hodges-Lehman estimator of difference between the pre- and post-impoundment period and percentage change relative to the pre-impoundment median with 95th percentage confidence intervals for all sites along the length of the Albert and Logan estuaries.

5. Discussion

5.1. Climate variability

Disentangling the complex interactions between human modifications and multiple stressors in natural systems presents a considerable challenge for managers. In the Logan-Albert estuary, turbidity and total nutrient concentrations showed strong seasonal variation. Higher turbidity and TP concentrations in the wet season are likely to be linked to elevated gully and sheet erosion in catchments, with phosphorus adsorbed to the sediments transported into the channel (Webster et al., 2001). Increased erosion may also explain elevated TN concentrations in the wet season, as sediment has a component that is particulate nitrogen (Garzon-Garcia et al., 2015). The highly seasonal rainfall regime in subtropical Australia ensures that the majority of nutrient and sediment loads are delivered from diffuse sources during the wet season, while nutrients tend to build-up on land during the dry season (Abal et al., 2005; Eyre, 1998).

The large increase in median turbidity in the mid Logan estuary between Chainages 17.4 km (42 NTU) and 23 km (110 NTU) is likely to reflect the location of an estuarine turbidity maximum (Fig. 3). It is important to note, however, that there has been substantial urbanisation along these reaches during the study period, which may have increased sediment loads and consequentially increased turbidity. Typically, the location of the estuarine turbidity maximum is largely dependent on the inflow conditions and tidal straining (Toublanc et al., 2016; Uncles et al., 2006). Mirfenderesk and Tomlinson (2006) showed strong tidal asymmetry in the Logan estuary, with flood currents exceeding those of ebb currents and longer low-water slack periods than high-water slack periods. Strong mixing processes and long periods of low flow lead to a predominantly well-mixed estuary for the much of the year. In well-mixed estuaries like the Logan, tidal straining resulting from tidal asymmetry is generally the major cause of estuarine circulation (Burchard and Schuttelaars, 2012). The mixing maintains elevated levels of sediments and nutrients in the water column, despite little replenishment of sediment from the catchment during the dry season.

In subtropical estuaries, flushing times during low-flow periods tend to be very long (Eyre, 1998) and can lead to a build-up of in-stream nutrients and turbidity, particularly if there are important point-source contributions. The two WWTPs represent such point-sources, and NH_4-N concentrations rise considerably during the dry season when dilution of the WWTP discharge is reduced (Fig. 3). Concentrations of NH_4-N in the upper Logan estuary were similar to those at the river mouth, indicating that diffuse source contributions were likely to be negligible during the dry season. The influence of the WWTPs is also evident on FRP

concentrations, which typically peaked during the dry season at monitoring sites downstream of the WWTPs (Fig. 3). FRP:TP and NO_x-N:TN ratios were greater downstream and near to the WWTP during the dry season when dilution from streamflow was reduced. This suggests that the WWTPs predominantly remove particulates and perform denitrification, leaving relatively high FRP in the absence of specific additional treatment (e.g., biological and/or chemical P removal). High-flow periods decrease flushing times and increase dilution from catchment sources, reducing the influence of the WWTPs (Paerl et al., 2006). However, high-flow periods also bring significant diffuse loads and can change the nature of the estuary from well-mixed to partially mixed (Eyre, 1998), promoting flocculation at the freshwater-saltwater interface, which is seen to vary with the seasons (Fig. 3). As high flows push the saltwater further downstream, upstream stations change from being largely estuarine to more closely reflecting the catchment runoff composition.

Weather cycles (e.g., El Niño or La Niña) and extreme events are major influences on water quality (Wetz and Yoskowitz, 2013), including in subtropical Australia. Over the 15-year duration of the study, the predominant weather changed from extended drought to wetter conditions, which coincided with the impoundment of Wyaralong Dam in December 2010. Ideally, a flow adjustment technique could be adopted to remove the variance associated with streamflow and indicate whether changes in turbidity and nutrient concentrations were weather related. However, traditional techniques require a relationship between the water quality variable and discharge, and necessitate a stationary streamflow distribution (Hirsch et al., 1991), which due to the reservoir impoundment is not appropriate in this case. In recent years a number of techniques for trend analysis have been developed (e.g., Hirsch et al., 2010, Murphy et al., 2019), which include flow-normalisation techniques, and characterisation of non-linear changes and non-stationarity in time series data.

Several studies have shown that drought events result in improved water quality as runoff from agricultural lands is reduced (Burkholder et al., 2006; Palmer and Montagna, 2015). However, in this case a reverse trend occurred as nutrient concentrations decreased considerably at many sites along both estuaries during the latter, wetter phase of the study (Table 1). Improvements were greatest along the upper portions of the Logan estuary and the lower sections of the Albert close to the WWTP. While these changes correlated with the impoundment of Wyaralong Dam for the Logan estuary, no other major anthropogenic changes were identified in the Albert catchment during the study period. We therefore attribute this improvement principally to a change in climate. During the drought, low inflows and long residence times led to a build-up of nutrients in the estuary, mostly from the WWTP, while

during wetter conditions these nutrients tended to be flushed from the system. Similar patterns have been noted for the Hudson (Howarth et al., 2000) and Neuse (Paerl et al., 2006) estuaries in the United States during drought events. Furthermore, prolonged drought allows for a build-up of nutrients within soils and can lead to a loss riparian vegetation that could mitigate nutrient losses to the aquatic system (Bond et al., 2008; Drewry et al., 2009). In drought-impacted catchments these factors can allow for larger quantities of sediments and nutrients to be transported during storm events.

5.2. Wastewater discharges

During the study period effluent TN and TP loads from the Albert WWTP either increased or remained unchanged (Fig. 6), though concentrations near to and downstream of the WWTP decreased significantly ($p<0.01$; Table 1). The elevated streamflow and increased flushing during the latter half of the study is considered to be a major factor contributing to reduced TN, TP, and NO_x-N concentrations in the lower Albert estuary. Interestingly despite decreased effluent NH_4-N loads and increased streamflow, NH_4-N concentrations near to the WWTP did not decrease significantly (Table 1). This may be due to the tidal influence of the Logan estuary leading to a net influx of nutrients into the Albert. TN, TP and NH_4-N loads from the Logan WWTP all decreased during the study period (Fig. 6), which in combination with elevated streamflow, is presumably the predominant cause of the significant ($p<0.01$) decreases in NH_4-N, TN, and TP concentrations in the mid estuary.

5.3. Damming

Our hypothesis was that the impoundment of Wyaralong Dam in December 2010 would have positive implications for downstream water quality. This hypothesis was validated using the BACI test, which showed significant ($p<0.01$) decreases for turbidity, TP, FRP, and NO_x-N at the upper Logan estuary site (impact) relative to the upper Albert site (control; Table 2). For TN, however, the relative change in concentration at the impact and control sites was of a similar magnitude (Table 3), which suggests that climatic factors had a greater effect on TN than dam impoundment. Additionally, no effect of impoundment was found on NH_4-N concentrations, which may be explained by the relatively low concentrations found at the impact site (Logan River Chainage 33 km) in the pre-impoundment period (Fig. 3; concentrations at upstream sites are approximately an order of magnitude lower than those at sites near the WWTP), and the well oxidised state of the water in the upper estuary, which allows for rapid oxidisation of NH_4-N to nitrite and nitrate. The fact that both FRP and NO_x-N

concentrations decreased significantly post-impoundment at the impact site suggests that longer residence times in the dam may have resulted in greater biological uptake by phytoplankton than would have otherwise occurred under the earlier natural stream conditions.

In the São Francisco estuary, Medeiros et al. (2011) found similar improvements in downstream water quality due to the construction of several upstream dams. Jeong et al. (2014) reported that an estuary dam along the Geum River in Korea acted as a sink for both phosphate and ammonium, though water quality declined both above and below the reservoir during their study. In contrast, Baldwin et al. (2010) reported that there was net export of TN and TP, principally in the form of phytoplankton biomass, during a period of extreme drawdown from Lake Hume in southeast Australia, but the lake acted as a net sink of NO_x-N. Similarly, Westhorpe et al. (2015) investigated the effects of the Lake Copeton Dam, Australia, using a longitudinal profile of downstream sites, finding that the dam was a source of both nitrogen and phosphorus. They speculated that the release of water from the anaerobic zone of the lake elevated concentrations of NO_x-N and FRP downstream of the reservoir, with the additional NO_x-N likely arising from oxidation of NH_4-N.

Water can be released from any level of Wyaralong Dam , with releases of deeper waters likely to be avoided if there is a risk of anoxic water occurring immediately downstream of the dam. The studies by Baldwin et al. (2010) and Westhorpe et al. (2015) were conducted more than 40 years after construction of each reservoir to their respective studies, and the results may therefore reflect the reduced capacity of the reservoirs to trap sediments and particulate nutrients, as bottom sediments build-up and reservoir capacity diminishes. The Conowingo Dam upstream of Chesapeake Bay, for instance, has begun to export more sediment and phosphorus loads downstream due to reduced trapping capacity (Zhang et al., 2013; Zhang et al., 2016). However, Wyaralong Dam, completed in 2010 to supplement the regions water supply, is likely to initially have high capacity for sediment and nutrient trapping. Negative effects of dams arise from hindering migratory fish species and loss of riverine habitat and biodiversity. Globally, dam impoundment has been shown to decrease fish biodiversity (Liermann et al., 2012). In Australia, Kingsford (2000) showed dams have significant negative impacts on downstream floodplain wetlands, including reduced vegetation health and declines in bird, fish, and invertebrate populations. The Logan-Albert rivers discharge into southern Moreton Bay which is an ecologically significant Ramsar-listed site. Impacts of the dam at this broader scale on local ecology requires further study and quantification.

5.4. Future issues

Future climatic and land use changes projected for the southeast Queensland region (Low Choy et al., 2010; Suppiah et al., 2007) may negate any of the positive implications associated with the dam. The catchment is projected to urbanise significantly in the coming decades with an additional 200,000 residents predicted to live in the Logan City area by 2036 compared to 2011 (Queensland Government Statistician's Office, 2018). Increased effluent from WWTPs and runoff from urban areas may result in further increases to in-stream concentrations, particularly during the low-flow periods, and may necessitate WWTP upgrades or catchment offset schemes to accommodate the additional population. The duration and magnitude of low-flow periods could extend in the future as more prolonged and intense droughts are predicted with climate change for this region (Dai, 2013; Naumann et al., 2018). Effects of urbanisation and drought may therefore act synergistically to increase nutrient levels in the estuaries and cause eutrophication. Additionally, more intense precipitation (Groisman et al., 2005) and larger floods in subtropical regions (Eccles et al., 2019) will likely increase diffuse loads from storm events to the estuary. While Wyaralong Dam currently appears to reduce loads of nutrients and sediments delivered to the downstream river and estuary of the Albert, if the trapping capacity of the dam decreases in the future then it may not continue to act as a sediment and nutrient sink.

In order to better determine changes to water quality a more targeted monitoring regime may be required with more finely resolved sampling around key sites (near to Dam and WWTPs). Monitoring in the freshwater sections of the river is sparser, both temporally and spatially, than in the estuary. Improved monitoring along freshwater reaches would allow for factors relating to land use and climate change to be more easily determined and detached from that of the estuary.

6. Conclusion

Determining the principal drivers of water quality is especially challenging for estuaries where there are complex interactions between climate, tide, and anthropogenic factors. The long-term monitoring of key water quality constituents at appropriate spatial coverage allows for improved understanding of the factors contributing to changes in estuarine water quality. Analysis of the long-term trends and patterns of key water quality constituents in the subtropical Logan-Albert estuary, Australia revealed distinct differences between the two estuaries, with higher values and greater variability along the Logan estuary. Water quality trends also showed large spatial variability throughout the estuary, with significant decreases

along the upper Logan estuary and the lower Albert estuary over the duration of the study. Significant decreases in TP, FRP, NO_x-N concentrations and turbidity in the upper Logan estuary were principally attributed to the impoundment of Wyaralong Dam, which acted as a nutrient and sediment sink. Significant decreases in nutrient concentrations along the lower Albert estuary were mostly attributed to wetter conditions over the study period, leading to increased dilution of a major point-source load from the WWTP. We demonstrated how to tease apart these factors but also found constraints from the multiple interacting factors that made it difficult to isolate any one cause and its effect. Improved coverage of water quality monitoring along freshwater reaches would allow future studies to more easily differentiate between longer term climate variability and short-term changes relating to WWTP improvements and the development of Wyaralong Dam.

Acknowledgements

The first author received a Griffith University Postgraduate Research Scholarship.

References

Abal, E.G., Dennison, W.C., Bunn, S.E., 2005. Healthy waterways healthy catchment: making the connection in south east Queensland, Australia. Moreton Bay Waterways and Catchment Partnership, Brisbane.

American Public Health Association, 1998. Standard methods for the examination of water and wastewater, twentieth ed. American Public Health Association, Washington D.C.

Baldwin, D.S., Wilson, J., Gigney, H., Boulding, A., 2010. Influence of extreme drawdown on water quality downstream of a large water storage reservoir. River Res. Appl. 26, 194-206. DOI:https://doi.org/10.1002/rra.1255

Bertone, E., Stewart, R.A., Zhang, H., O'Halloran, K., 2015. Analysis of the mixing processes in the subtropical Advancetown Lake, Australia. J. Hydrol. 522, 67-79. DOI:https://doi.org/10.1016/j.jhydrol.2014.12.046

Bond, N.R., Lake, P.S., Arthington, A.H., 2008. The impacts of drought on freshwater ecosystems: an Australian perspective. Hydrobiologia 600, 3-16. DOI:https://doi.org/10.1007/s10750-008-9326-z

Bunn, S., Abal, E., Greenfield, P., Tarte, D., 2007. Making the connection between healthy waterways and healthy catchments: South East Queensland, Australia. Water Supp. 7, 93-100. DOI:https://doi.org/10.2166/ws.2007.044

Burchard, H., Schuttelaars, H.M., 2012. Analysis of tidal straining as driver for estuarine circulation in well-mixed estuaries. J. Phys. Oceanogr. 42, 261-271. DOI:https://doi.org/10.1175/JPO-D-11-0110.1

Burkholder, J.M., Dickey, D.A., Kinder, C.A., Reed, R.E., Mallin, M.A., McIver, M.R., Cahoon, L.B., Melia, G., Brownie, C., Smith, J., 2006. Comprehensive trend analysis of nutrients and related variables in a large eutrophic estuary: a decadal study of anthropogenic and climatic influences. Limnol. Oceanogr. 51, 463-487. DOI:https://doi.org/10.4319/lo.2006.51.1_part_2.0463

Chang, H.-Y., Chiu, M.-C., Chuang, Y.-L., Tzeng, C.-S., Kuo, M.-H., Yeh, C.-H., Wang, H.-W., Wu, S.-H., Kuan, W.-H., Tsai, S.-T., Shao, K.-T., Lin, H.-J., 2017. Community responses to dam removal in a subtropical mountainous stream. Aquat. Sci. 79, 967-983. DOI:https://doi.org/10.1007/s00027-017-0545-0

Dąbrowska, J., Bawiec, A., Pawęska, K., Kamińska, J., Stodolak, R., 2017. Assessing the impact of wastewater effluent diversion on water quality. Pol. J. Environ. Stud. 26, 9-16. DOI:https://doi.org/10.15244/pjoes/64748
Dai, A., 2013. Increasing drought under global warming in observations and models. Nat. Clim. Change 3, 52-58. DOI:https://doi.org/10.1038/nclimate1633
Dennison, W.C., Abal, E.G., 1999. Moreton Bay study: a scientific basis for the healthy waterways campaign. South East Qld Regional Water Quality Management Strategy Team.
Department of Environment and Heritage Protection (DEHP), 2015. Wetland Info. https://wetlandinfo.ehp.qld.gov.au/wetlands/assessment/monitoring/point-source-release/sewage-treatment-facilities/ (Accessed February 2019).
Department of Infrastructure and Transport, 2013. Population growth, jobs growth and commuting flows in South East Queensland. Commonwealth of Australia, Canberra.
Department of Science Information Technology Innovation and the Arts (DSITIA), 2014. Land Use Summary 1999-2012 for the Logan-Albert catchment within SEQ, Brisbane.
Drewry, J.J., Newham, L.T.H., Croke, B.F.W., 2009. Suspended sediment, nitrogen and phosphorus concentrations and exports during storm-events to the Tuross estuary, Australia. J. Environ. Manage. 90, 879-887. DOI:https://doi.org/10.1016/j.jenvman.2008.02.004
Eccles, R., Zhang, H., Hamilton, D., 2019. A review of the effects of climate change on riverine flooding in subtropical and tropical regions. J. Water Clim. Change 10, 687-707. DOI:https://doi.org/10.2166/wcc.2019.175
Ecosystem Health Monitoring Program, 2007. Ecosystem Health Monitoring Program 2006-07 Annual Technical Report, in: Partnership, S.E.Q.H.W. (Ed.), Brisbane.
Eyre, B., 1998. Transport, retention and transformation of material in Australian estuaries. Estuaries 21, 540-551. DOI:https://doi.org/10.2307/1353293
Friedl, G., Wüest, A., 2002. Disrupting biogeochemical cycles - Consequences of damming. Aquat. Sci. 64, 55-65. DOI:https://doi.org/10.1007/s00027-002-8054-0
Garzon-Garcia, A., Olley, J.M., Bunn, S.E., 2015. Controls on carbon and nitrogen export in an eroding catchment of south-eastern Queensland, Australia. Hydrol. Process. 29, 739-751. DOI:https://doi.org/10.1002/hyp.10192
Groisman, P.Y., Knight, R.W., Easterling, D.R., Karl, T.R., Hegerl, G.C., Razuvaev, V.N., 2005. Trends in intense precipitation in the climate record. J. Clim. 18, 1326-1350. DOI:http://dx.doi.org/10.1175/JCLI3339.1
Harris, G.P., 2001. Biogeochemistry of nitrogen and phosphorus in Australian catchments, rivers and estuaries: effects of land use and flow regulation and comparisons with global patterns. Mar. Freshwater Res. 52, 139-149. DOI:https://doi.org/10.1071/MF00031
Hirsch, R.M., Alexander, R.B., Smith, R.A., 1991. Selection of methods for the detection and estimation of trends in water quality. Water Resour. Res. 27, 803-813. DOI:https://doi.org/10.1029/91WR00259
Hirsch, R.M., Moyer, D.L., Archfield, S.A., 2010. Weighted Regressions on Time, Discharge, and Season (WRTDS), with an Application to Chesapeake Bay River Inputs. J. Am. Water Resour. As. 46, 857-880. DOI:10.1111/j.1752-1688.2010.00482.x
Hirsch, R.M., Slack, J.R., Smith, R.A., 1982. Techniques of trend analysis for monthly water quality data. Water Resour. Res. 18, 107-121. DOI:https://doi.org/10.1029/WR018i001p00107
Hodges Jr, J.L., Lehmann, E.L., 1963. Estimates of location based on rank tests. Ann. Math. Stat. 34, 598-611. DOI:https://www.jstor.org/stable/2238406
Howarth, R.W., Swaney, D.P., Butler, T.J., Marino, R., 2000. Rapid communication: climatic control on eutrophication of the Hudson River Estuary. Ecosystems 3, 210-215. DOI:https://doi.org/10.1007/s100210000020
Hughes, A.O., Quinn, J.M., 2014. Before and after integrated catchment management in a headwater catchment: Changes in water quality. Environ. Manage. 54, 1288-1305. DOI:https://doi.org/10.1007/s00267-014-0369-9
Jeong, Y.H., Yang, J.S., Park, K., 2014. Changes in water quality after the construction of an estuary dam in the geum river estuary dam system, korea. J. Coast. Res. 30, 1278-1286. DOI:https://doi.org/10.2112/JCOASTRES-D-13-00081.1

Kingsford, R.T., 2000. Ecological impacts of dams, water diversions and river management on floodplain wetlands in Australia. Austral Ecol. 25, 109-127. DOI:https://doi.org/10.1046/j.1442-9993.2000.01036.x
Li, D., Lu, X.X., Yang, X., Chen, L., Lin, L., 2018. Sediment load responses to climate variation and cascade reservoirs in the Yangtze River: A case study of the Jinsha River. Geomorphology 322, 41-52. DOI:https://doi.org/10.1016/j.geomorph.2018.08.038
Liermann, C.R., Nilsson, C., Robertson, J., Ng, R.Y., 2012. Implications of dam obstruction for global freshwater fish diversity. Bioscience 62, 539-548. DOI:https://doi.org/10.1525/bio.2012.62.6.5
Low Choy, D., Baum, S., Serrao-Neumann, S., Crick, F., Sanò, M., Harman, B., 2010. Climate change vulnerability in South East Queensland: A spatial and sectoral assessment, Unpublished report for the South East Queensland Climate Adaptation Research Initiative, Griffith University.
Malmqvist, B., Rundle, S., 2002. Threats to the running water ecosystems of the world. Environ. Conserv. 29, 134-153. DOI:https://doi.org/10.1017/S0376892902000097
Martina, L.C., Principe, R., Gari, N., 2013. Effect of a dam on epilithic algal communities of a mountain stream: Before-after dam construction comparison. J. Limnol. 72, 79-94. DOI:https://doi.org/10.4081/jlimnol.2013.e7
Medeiros, P.R.P., Knoppers, B.A., Cavalcante, G.H., de Souza, W.F.L., 2011. Changes in nutrient loads (N, P and Si) in the São Francisco estuary after the construction of dams. Braz. Arch. Biol. Techn. 54, 387-397. DOI:http://dx.doi.org/10.1590/S1516-89132011000200022
Mirfenderesk, H., Tomlinson, R., 2006. Tidal asymmetry in a prodominantly semidiurnal regieme estuary (case study-Logan River), 7th International Conference on HydroScience and Engineering, Philadelphia, USA.
Molina-Navarro, E., Andersen, H.E., Nielsen, A., Thodsen, H., Trolle, D., 2018. Quantifying the combined effects of land use and climate changes on stream flow and nutrient loads: A modelling approach in the Odense Fjord catchment (Denmark). Sci. Total Environ. 621, 253-264. DOI:https://doi.org/10.1016/j.scitotenv.2017.11.251
Murphy, R.R., Perry, E., Harcum, J., Keisman, J., 2019. A Generalized Additive Model approach to evaluating water quality: Chesapeake Bay case study. Environ. Model. Software 118, 1-13. DOI:https://doi.org/10.1016/j.envsoft.2019.03.027
National Land and Water Resources Audit, 2001. Australian agriculture assessment 2001: volume 1, Canberra.
National Pollutant Inventory, 2019. http://www.npi.gov.au/ (Accessed February 2019).
Naumann, G., Alfieri, L., Wyser, K., Mentaschi, L., Betts, R.A., Carrao, H., Spinoni, J., Vogt, J., Feyen, L., 2018. Global Changes in Drought Conditions Under Different Levels of Warming. Geophys. Res. Lett. 45, 3285-3296. DOI:https://doi.org/10.1002/2017GL076521
Nunes, J., Seixas, J., Keizer, J., Ferreira, A., 2009. Sensitivity of runoff and soil erosion to climate change in two Mediterranean watersheds. Part II: assessing impacts from changes in storm rainfall, soil moisture and vegetation cover. Hydrol. Process. 23, 1212-1220. DOI:https://doi.org/10.1002/9781444328455.ch15
Olley, J., Burton, J., Hermoso, V., Smolders, K., McMahon, J., Thomson, B., Watkinson, A., 2015. Remnant riparian vegetation, sediment and nutrient loads, and river rehabilitation in subtropical Australia. Hydrol. Process. 29, 2290-2300. DOI:https://doi.org/10.1002/hyp.10369
Paerl, H.W., Valdes, L.M., Piehler, M.F., Stow, C.A., 2006. Assessing the effects of nutrient management in an estuary experiencing climatic change: the Neuse River Estuary, North Carolina. Environ. Manage. 37, 422-436. DOI:https://doi.org/10.1007/s00267-004-0034-9
Palmer, T.A., Montagna, P.A., 2015. Impacts of droughts and low flows on estuarine water quality and benthic fauna. Hydrobiologia 753, 111-129. DOI:https://doi.org/10.1007/s10750-015-2200-x
Queensland Government Statistician's Office, 2018. Queensland regional profiles: Logan local government area,. Queensland Treasury.
Rabalais, N.N., Turner, R.E., Díaz, R.J., Justić, D., 2009. Global change and eutrophication of coastal waters. ICES J. Mar. Sci. 66, 1528-1537. DOI:https://doi.org/10.1093/icesjms/fsp047
Shrestha, M.K., Recknagel, F., Frizenschaf, J., Meyer, W., 2017. Future climate and land uses effects on flow and nutrient loads of a Mediterranean catchment in South Australia. Sci. Total Environ. 590-591, 186-193. DOI:https://doi.org/10.1016/j.scitotenv.2017.02.197

Smith, E.P., 2002. BACI design, in: El-Shaarawi, A.H., Piegorsch, W.W. (Eds.), Encyclopedia of Environmetrics. John Wiley & Sons, Chirchester, pp. 141-148. DOI:https://doi.org/10.1002/9781118445112.stat07659
Smokorowski, K., Randall, R., 2017. Cautions on using the Before-After-Control-Impact design in environmental effects monitoring programs. Facets 2, 212-232. DOI:https://doi.org/10.1139/facets-2016-0058
Stewart-Oaten, A., Murdoch, W.W., Parker, K.R., 1986. Environmental impact assessment: "Pseudoreplication" in time? Ecology 67, 929-940. DOI:https://doi.org/10.2307/1939815
Suppiah, R., Hennessy, K., Whetton, P., McInnes, K., Macadam, I., Bathols, J., Ricketts, J., Page, C., 2007. Australian climate change projections derived from simulations performed for the IPCC 4th Assessment Report. Aust. Meteorol. Mag. 56, 131-152.
Thompson, J., Pelc, C., Brogan III, W., Jordan, T., 2018. The multiscale effects of stream restoration on water quality. Ecol. Eng. 124, 7-18. DOI:https://doi.org/10.1016/j.ecoleng.2018.09.016
Tibbetts, I.B., Hall, N.J., Tibbetts, I.R., Dennison, W., 1999. Moreton bay and catchment. School of Marine Science, University of Queensland, Brisbane.
Toublanc, F., Brenon, I., Coulombier, T., 2016. Formation and structure of the turbidity maximum in the macrotidal Charente estuary (France): Influence of fluvial and tidal forcing. Estuar. Coast. Shelf Sci. 169, 1-14. DOI:https://doi.org/10.1016/j.ecss.2015.11.019
Uncles, R.J., Stephens, J.A., Harris, C., 2006. Runoff and tidal influences on the estuarine turbidity maximum of a highly turbid system: The upper Humber and Ouse Estuary, UK. Mar. Geol. 235, 213-228. DOI:https://doi.org/10.1016/j.margeo.2006.10.015
van Dijk, A.I., Beck, H.E., Crosbie, R.S., de Jeu, R.A., Liu, Y.Y., Podger, G.M., Timbal, B., Viney, N.R., 2013. The Millennium Drought in southeast Australia (2001–2009): Natural and human causes and implications for water resources, ecosystems, economy, and society. Water Resour. Res. 49, 1040-1057. DOI:https://doi.org/10.1002/wrcr.20123
Walling, D., Fang, D., 2003. Recent trends in the suspended sediment loads of the world's rivers. Global Planet. Change 39, 111-126. DOI:https://doi.org/10.1016/S0921-8181(03)00020-1
Webster, I.T., Ford, P.W., Hancock, G., 2001. Phosphorus dynamics in Australian lowland rivers. Mar. Freshwater Res. 52, 127-137. DOI:https://doi.org/10.1071/MF00037
Westhorpe, D.P., Mitrovic, S.M., Growns, I.O., Hadwen, W.L., Rees, G.N., 2015. Disruption in water quality patterns along the river continuum by a large bottom release dam. Australas. J. Env. Man. 22, 400-416. DOI:https://doi.org/10.1080/14486563.2014.999133
Wetz, M.S., Yoskowitz, D., 2013. An 'extreme'future for estuaries? Effects of extreme climatic events on estuarine water quality and ecology. Mar. Pollut. Bull. 69, 7-18. DOI:https://doi.org/10.1016/j.marpolbul.2013.01.020
Zhang, Q., Brady, D.C., Ball, W.P., 2013. Long-term seasonal trends of nitrogen, phosphorus, and suspended sediment load from the non-tidal Susquehanna River Basin to Chesapeake Bay. Sci. Total Environ. 452-453, 208-221. DOI:https://doi.org/10.1016/j.scitotenv.2013.02.012
Zhang, Q., Hirsch, R.M., Ball, W.P., 2016. Long-term changes in sediment and nutrient delivery from Conowingo dam to Chesapeake Bay: effects of reservoir sedimentation. Environ. Sci. Technol. 50, 1877-1886. DOI:https://doi.org/10.1021/acs.est.5b04073

Supplementary Materials:

S1. Boxplots of TN, TP, and turbidity at key monitoring sites

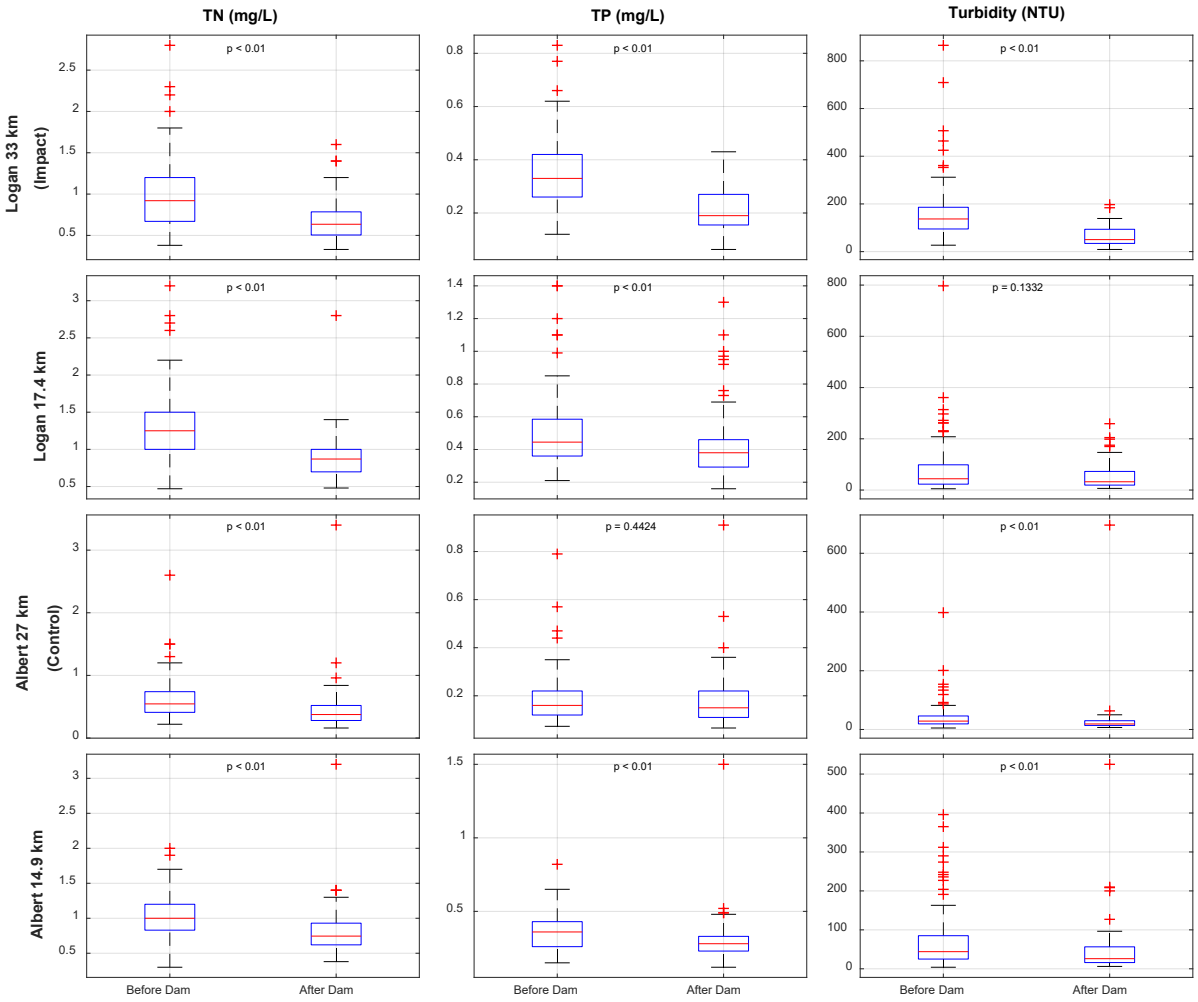

Fig. S1. Boxplots comparing the distribution of TN, TP, and turbidity in the pre- and post-impoundment periods and p-values from the Wilcoxon Rank-Sum test showing significant differences at upper Logan and Albert estuary sites (Chainage 33 and 27 km, respectively) and sites near to WWTPs (Chainage 17.4 and 14.9 km for Logan and Albert estuaries, respectively).

S2. GAM Model

In addition to analysing trends using the seasonal Mann-Kendall test, a Generalised Additive Model (GAM) approach (Murphy et al., 2019) was applied using the 'baytrends' package in the R statistical software (Murphy et al., 2020), in which the GAMs are fit using the 'mgcv' package (Wood, 2019). The structure of the GAM is presented below in 'mgcv' syntax below.

gam2: gam(y ~ cyear + s(cyear, k = c*(10,2/3)*) + s(doy,bs = 'cc') + ti(cyear,doy,bs = ('tp','cc')), knots = list(doy = c(1,366)), select= TRUE)

Where: *y* is a response variable, *cyear* is the zero-centred date in decimal form, *doy* is the day of year, *s()* is a spline, *ti()* is a tensor product, *k* is the number of knots (either 10 or 2/3*number of years), *bs='tp'* signifies a penalised thin plate regression, while *bs='cc'* signifies a cyclic penalized cubic regression spline (Murphy et al., 2019). The structure of the model allows for non-linear trends and seasonal cycles that can vary over time.

In addition, to the gam2 model, the gam4 model was considered, which considered inter-annual variations in streamflow. Streamflow data from the Yarrahappini and Bromfleet stream gauges (ID: 145014A and 145102B) located upstream on the Logan and Albert rivers, respectively were adopted in this analysis. Streamflow was averaged over a period *n* preceding day (*flw_sal*), where *n* was determined by comparing correlation coefficients (Murphy et al., 2019).

gam4: gam(y ~ cyear + s(cyear, k = c*(10,1/3)*) + s(doy,bs = 'cc') + ti(cyear,doy,bs = c('tp','cc')) + s(flw_sal,k = c*(10,2/3)*) + ti(flw_sal,doy,bs = c('tp','cc')) + ti(flw_sal, cyear,bs = c('tp','tp')) + ti(flw_sal,doy,cyear, bs = c('tp','cc','tp')), knots = list(doy = c(1,366)), select = TRUE)

Trends from GAM models were determined by evaluating the percentage change between the model estimates at beginning and end of the study period and the significance level of this change (Murphy et al., 2019). The number of years selected at the beginning and end of the period is an important consideration, though selection of the most appropriate number of years is not always clear. Too many years may underestimate a trend in the data, while too few years may be overly influenced by year-to-year variations in streamflow and water quality. This is a particular issue in subtropical Australia, where rivers are subject to highly variable flow and water quality regimes. As such, we chose to evaluate periods of 4 and 7 years at the beginning and end of the GAM models, the results for which are presented below.

Table S1. Percentage change results based on the GAM (4-years). Green colours denote decreasing trends and red increasing. Bold values indicate significant ($p<0.01$) trends.

Site (km)	TN	TP	Turbidity	NH_4-N	NO_x-N	FRP
Logan 0	20.1	6.9	24.2	35.3	0.9	**-33.8**
Logan 2	5.8	-7.5	47.6	-10.4	-35.1	**-41.5**
Logan 4.8	-5.2	-6.3	21.9	-0.5	**-51.4**	-18.6
Logan 7.8	-14.6	-16.0	24.8	-3.1	**-49.7**	**-17.2**
Logan 11.1	**-22.5**	**-23.5**	-15.6	-8.3	**-47.2**	**-23.3**
Logan 13.3	**-27.1**	**-28.9**	-13.8	-23.9	**-47.4**	**-23.5**
Logan 15.6	**-33.4**	**-36.7**	-6.6	-36.6	**-58.4**	**-39.4**
Logan 17.4	**-40.9**	**-35.2**	-22.3	**-48.2**	**-61.4**	**-37.3**
Logan 23	**-51.7**	**-53.0**	**-50.4**	**-69.8**	**-80.0**	**-55.2**
Logan 26.3	**-51.1**	**-53.4**	**-51.9**	**-72.8**	**-87.2**	**-55.9**
Logan 29.3	**-46.2**	**-51.8**	**-54.8**	-49.6	**-88.0**	**-53.5**
Logan 33	**-42.8**	**-51.5**	**-58.7**	-32.5	**-84.4**	**-49.0**
Albert 11.1	**-25.9**	**-33.4**	-21.2	-19.7	**-44.8**	**-25.4**
Albert 13.1	**-28.6**	**-32.1**	-20.9	-28.6	**-45.4**	**-33.5**
Albert 14.9	**-31.6**	**-29.7**	-24.7	-46.2	**-45.6**	**-25.5**
Albert 16.9	**-25.2**	**-21.2**	-19.7	-26.5	**-54.8**	**-17.8**
Albert 21	**-30.9**	**-18.0**	-28.4	-22.7	-50.1	-2.8
Albert 23.1	**-33.8**	-16.0	-30.4	-42.8	-33.4	9.0
Albert 27	**-37.8**	-10.1	**-38.3**	**-59.2**	-52.5	**31.8**

Table S2. Percentage change based on the GAM (7-years). Green colours denote decreasing trends and red increasing. Bold values indicate significant ($p<0.01$) trends.

Site (km)	TN	TP	Turbidity	NH_4-N	NO_x-N	FRP
Logan 0	19.2	17.5	11.9	52.0	35.3	-9.2
Logan 2	10.4	6.0	26.0	17.2	-14.6	-18.5
Logan 4.8	-1.7	-4.2	6.7	9.4	**-40.2**	-3.5
Logan 7.8	-12.1	-9.0	0.9	-2.1	**-39.4**	-6.7
Logan 11.1	**-17.7**	**-17.5**	-22.2	-6.4	**-37.1**	**-13.5**
Logan 13.3	**-20.5**	**-18.7**	-21.1	-16.0	**-37.3**	**-12.0**
Logan 15.6	**-28.4**	**-28.0**	-6.0	-32.0	**-47.1**	**-29.2**
Logan 17.4	**-33.8**	**-20.1**	-18.6	**-42.9**	**-49.9**	**-23.1**
Logan 23	**-43.7**	**-45.0**	**-49.1**	**-54.1**	**-69.1**	**-45.3**
Logan 26.3	**-41.0**	**-45.5**	**-50.7**	**-51.3**	**-77.6**	**-46.0**
Logan 29.3	**-35.3**	**-43.9**	**-54.1**	-37.8	**-78.7**	**-42.9**
Logan 33	**-31.3**	**-43.4**	**-58.5**	-15.7	**-67.8**	**-41.1**
Albert 11.1	**-20.7**	**-25.2**	-24.8	-14.6	**-35.1**	**-15.8**
Albert 13.1	**-22.5**	**-24.5**	-24.0	-21.1	**-36.2**	**-22.2**
Albert 14.9	**-23.2**	**-18.3**	**-28.2**	-26.7	**-37.0**	**-14.8**
Albert 16.9	**-18.5**	**-15.0**	-26.5	-7.2	-34.1	-10.0
Albert 21	**-23.7**	-11.2	**-27.2**	-4.4	-31.9	0.9
Albert 23.1	**-25.9**	-10.1	**-29.1**	-32.0	-25.5	7.2
Albert 27	**-29.4**	-5.6	**-34.5**	**-47.3**	-41.2	**27.9**

Table S3. Percentage change results based on the GAM (4-years) with flow-adjusted. Green colours denote decreasing trends and red increasing. Bold values indicate significant ($p<0.01$) trends.

Site (km)	TN	TP	Turbidity	NH_4-N	NO_x-N	FRP
Logan 0	-3.0	**-22.6**	1.2	-44.5	**-57.2**	**-46.7**
Logan 2	-10.7	**-22.6**	23.3	**-52.1**	**-67.4**	**-54.5**
Logan 4.8	**-26.4**	**-23.0**	-1.1	**-53.2**	**-73.3**	**-32.5**
Logan 7.8	**-31.5**	**-22.4**	-6.6	-39.8	**-66.9**	-3.6
Logan 11.1	**-34.3**	**-30.0**	**-42.9**	-33.0	**-53.1**	-11.1
Logan 13.3	**-33.7**	**-23.8**	**-39.7**	-37.8	**-43.9**	-13.2
Logan 15.6	**-20.5**	**-22.7**	**-37.3**	-30.7	**-58.4**	**-23.6**
Logan 17.4	**-28.3**	**-20.9**	**-45.5**	-36.1	**-55.0**	-19.2
Logan 23	**-46.8**	**-43.3**	**-60.2**	**-65.8**	**-75.6**	**-36.5**
Logan 26.3	**-45.1**	**-35.7**	**-59.6**	**-67.2**	**-84.5**	**-33.4**
Logan 29.3	**-42.9**	**-41.0**	**-59.1**	**-59.8**	**-87.5**	**-36.9**
Logan 33	**-38.0**	**-35.3**	**-57.0**	-48.1	**-76.6**	**-30.8**
Albert 11.1	**-29.7**	**-32.6**	**-30.7**	-26.9	**-49.6**	10.5
Albert 13.1	**-25.7**	-17.0	-32.9	-31.0	**-40.0**	**-28.6**
Albert 14.9	**-28.3**	**-26.6**	-29.1	-41.8	**-45.8**	**-19.4**
Albert 16.9	12.1	**-18.4**	-20.9	-9.2	-42.2	-14.8
Albert 21	**-21.9**	-11.5	**-32.5**	-28.2	-19.1	2.9
Albert 23.1	**-25.4**	-7.2	**-30.7**	-44.2	-48.0	19.6
Albert 27	**-21.9**	-2.0	**-32.8**	**-59.8**	-62.1	34.5

Table S4. Percentage change results based on the GAM (7-years) with flow-adjusted. Green colours denote decreasing trends and red increasing. Bold values indicate significant ($p<0.01$) trends.

Site (km)	TN	TP	Turbidity	NH_4-N	NO_x-N	FRP
Logan 0	1.2	-2.8	-3.4	-26.5	-40.8	**-27.2**
Logan 2	-6.0	**-17.2**	12.8	-29.9	**-56.4**	**-35.7**
Logan 4.8	**-21.3**	**-14.8**	-10.5	**-40.1**	**-65.6**	**-20.3**
Logan 7.8	**-27.0**	**-14.7**	-21.4	**-33.6**	**-56.4**	2.0
Logan 11.1	**-28.5**	**-21.9**	**-41.7**	-29.1	**-47.7**	-3.3
Logan 13.3	**-26.8**	-12.7	**-40.8**	-31.3	**-38.8**	-1.7
Logan 15.6	**-22.6**	-13.3	**-33.5**	-30.2	**-47.1**	**-16.7**
Logan 17.4	**-26.5**	-5.6	**-40.5**	**-36.8**	**-44.3**	-5.0
Logan 23	**-39.0**	**-34.5**	**-56.7**	-34.2	**-64.1**	**-22.8**
Logan 26.3	**-36.2**	**-27.5**	**-54.4**	-37.9	**-73.5**	**-21.6**
Logan 29.3	**-32.6**	**-31.3**	**-52.3**	-42.7	**-75.7**	**-23.1**
Logan 33	**-29.2**	**-29.3**	**-54.3**	-36.9	**-58.9**	**-22.0**
Albert 11.1	**-26.0**	**-23.8**	**-37.4**	-22.4	**-44.3**	10.4
Albert 13.1	**-22.4**	-11.2	**-37.2**	-22.1	**-32.4**	**-16.7**
Albert 14.9	**-20.7**	**-14.1**	**-34.9**	-16.0	**-36.5**	-7.3
Albert 16.9	5.8	-9.8	**-31.0**	20.8	-33.4	-1.6
Albert 21	-10.3	-1.0	**-33.2**	-11.2	-6.4	11.3
Albert 23.1	-14.0	2.0	**-32.8**	-30.5	-38.0	**21.3**
Albert 27	-14.8	5.2	**-27.2**	**-53.2**	**-58.8**	**32.8**

References

Murphy, R.R., Perry, E., Harcum, J., Keisman, J., 2019. A Generalized Additive Model approach to evaluating water quality: Chesapeake Bay case study. Environ. Model. Software 118, 1-13. DOI:https://doi.org/10.1016/j.envsoft.2019.03.027
Murphy, R.R., Perry, E., Harcum, J., Keisman, J., Leppo, E.W., 2020. Baytrends. https://cran.r-project.org/web/packages/baytrends/index.html
Wood, S., 2019. Mgcv. https://CRAN.R-project.org/package=mgcv